

Sensitive Voltammetric Analysis of Cetirizine Using Electrochemical Sensor Based on Poly (methyl orange) Modified Carbon Nanotube Paste Electrode

Mohammed Monirul Islam^{1*}, Noor E Hafsa², Muhammad Muhitur Rahman³, MD Arifuzzaman⁴, and Sayeed Rushd⁵

¹ Department of Biomedical Sciences, College of Clinical Pharmacy, King Faisal University, Al-Ahsa, 31982, Saudi Arabia

² Department of Computer Science, College of Computer Science And Information Technology, King Faisal University, Al-Ahsa, 31982, Saudi Arabia

³ Department of Civil and Environmental Engineering, College of Engineering, King Faisal University, Al-Ahsa, 31982, Saudi Arabia

⁴ Department of Civil and Environmental Engineering, College of Engineering, King Faisal University, Al-Ahsa, 31982, Saudi Arabia

⁵ Department of Chemical Engineering, College of Engineering, King Faisal University, Al-Ahsa, 31982, Saudi Arabia

*E-mail: mislam@kfu.edu.sa

Received: 2 xxx 2021 / Accepted: 15 December 2021 / Published: 2 February 2022

Poly (methyl orange) was demonstrated as an effective polymer for the modification of electrode surface for the electrochemical investigation of various drug molecules. An efficient detection of cetirizine (CTZ), a renowned antihistamine drug is of great importance. Systematic analysis of CTZ was done through cyclic voltammetry (CV) method in phosphate buffer saline with pH 7.0 at 0.1 V/s scan rate. The developed poly(methyl orange) modified carbon nanotube electrode (PMO/CNTPE) was highly conductive and it was demonstrated through CV and electrochemical impedance spectroscopy methods. Under best possible investigational circumstances, the developed non-enzymatic sensing device was proficient to detect CTZ with a broad concentration range (2 μM to 45 μM) and produced lower limit of detection (0.076 μM). Additionally, the designed electrochemical sensor exhibited superior stability along with excellent repeatability and reproducibility showcasing its efficient sensing ability. The fabricated sensing device was inspected to check its applicability in the analysis of medicinal formulations with acceptable recovery.

Keywords: Cetirizine, poly(methyl orange), multi walled carbon nanotubes, tablet sample analysis

1. INTRODUCTION

Analysis of drug moieties is of great concern in the field of quality control. Hence, the advancement of uncomplicated, highly responsive, swift and reliable mode for the electrochemical investigation of drug molecules is very significant. Cetirizine dihydrochloride (CTZ) is an effective and highly accepted antihistamine drug widely utilized to cure and prevent various allergic reactions in the human body [1, 2]. It is also used to treatment asthma patients. On the other hand, the overuse of this medicine causes dry mouth, constipation, headache, blurred vision, drowsiness and dizziness [3].

Various analytical techniques have been already reported for the qualitative and quantitative analysis of CTZ. Some of those techniques are liquid chromatography-mass spectrometry [4], high performance thin layer chromatography [5], thin layer chromatography-densitometry [6], high performance liquid chromatography [7], spectrophotometry [8], gas chromatography [9], capillary zone electrophoresis [10], LC-tandem mass spectrometry [11], and electrochemical investigation with different modified electrodes [12, 13]. In contrast to other methods, electroanalytical methods entail low priced instrumentation, less time consuming, less requirement of solvent and it does not necessitate any sample pre-treatment procedure [14–18].

Multiwalled carbon nanotubes (MWCNTs) have fascinated mammoth interest in the current era owing to their large surface area, distinctive electronic features, high chemical stability and conductivity. As an electrode material it facilitate the exchange of electrons between the sensor and the molecule under study and it afford a novel surface for designing a new sensing device through modification [19–23].

The alteration of sensing surface by means of electropolymerization of organic dyes provides a conducting surface for the sensing of electroactive and bioactive molecules. Due to electropolymerization, a uniform polymer layer was formed on the electrode surface which directs the transfer of charge. These altered electrode surface offers electrocatalytic and antifouling properties and also it avoids unfavourable reaction with the electrode substance [24–26].

In this piece of work, methyl orange (MO) was electropolymerized over the MWCNTs paste electrode surface for the sensing of CTZ. The poly(MO) modified carbon nanotube paste electrode (PMO/CNTPE) displayed enhanced sensing performance than bare carbon nanotube paste electrode (BCNTPE) and the surfaces characteristics were studied using cyclic voltammetry (CV), electrochemical impedance spectroscopy (EIS) and field emission scanning electron spectroscopy (FE-SEM). The designed electrode was also applied to analyse pharmaceutical samples with adequate recovery.

2. MATERIALS AND METHODS

2.1 Reagents and solutions

All the chemical used for this research work is of analytical reagent grade. CTZ, PCM and MO were procured from Sigma. The binder (Silicone oil) and KCl were obtained from Merk chemicals. Sodium dihydrogen phosphate (NaH_2PO_4) and disodium hydrogen phosphate (Na_2HPO_4) were purchased from Sigma. MWCNTs (10–30 μm length, external diameter 30–50 nm) were procured from

Sigma. The standard redox probe $K_4[Fe(CN)_6] \cdot 3H_2O$ was procured from Sigma-Aldrich, India. CTZ tablet sample was purchased from the local medical store.

The solutions of MO, CTZ, PCM, $K_4[Fe(CN)_6]$, KCl, NaH_2PO_4 and Na_2HPO_4 of required concentration were prepared by dissolving the calculated amount of solute in double distilled water. Phosphate buffer saline (PBS) of various pH were prepared by intermixing the calculated volume of 0.2 M NaH_2PO_4 and Na_2HPO_4 .

2.2 Instrumentation

The electrochemical analyser was used for the electrochemical investigation. This equipment was connected to an electrolytic cell bearing tri-electrode setup with a reference electrode (calomel electrode), an auxiliary electrode (Pt wire) and a working electrode (BCNTPE, PMO/CNTPE). The CV data were collected in a computer system connected to an electrochemical analyser. The complete investigation was executed at laboratory temperature (25 ± 2 °C).

2.3 Development of BCNTPE

The paste of MWCNTs necessary for the development of working electrode was prepared by intermixing the MWCNTs and silicone oil in the proportion of 60:40 using an agate mortar and it was firmed using a pestle. Thus the prepared paste was packed into the hollow space of Teflon rod (3 mm internal diameter) and its exterior was massaged over the tissue paper to accomplish the uniform surface. This prepared Teflon tube was used as BCNTPE. Then the electrical contact between the electrode and the electrochemical analyser was achieved by the inclusion of copper wire at the other end of the electrode.

2.4 Preparation of PMO/CNTPE

The PMO/CNTPE was prepared by the method of electro-polymerization of MO on the BCNTPE surface through CV technique. It was done by scanning the BCNTPE surface in an electrolytic cell containing PBS of pH 7.0 with 1 mM MO for 10 multiple cycles within the potential range of -0.6 to 1.4 V at a scan rate of 0.1 V/s. During this process of electropolymerization the current value enhances progressively with the increase of number of polymerization cycles indicates the development of poly(MO) layer on the BCNTPE surface. The cyclic voltammograms (CVs) produced during this process is shown in Fig. 1. The conductive layer of poly(MO) developed on the BCNTPE surface enhances the sensing ability of the electrode for the electroanalysis of target analyte. After completion of this process the exterior of the electrode was rinsed with double distilled water to eradicate the unreacted monomers. The polymer form of MO is shown in the inset of Fig. 1.

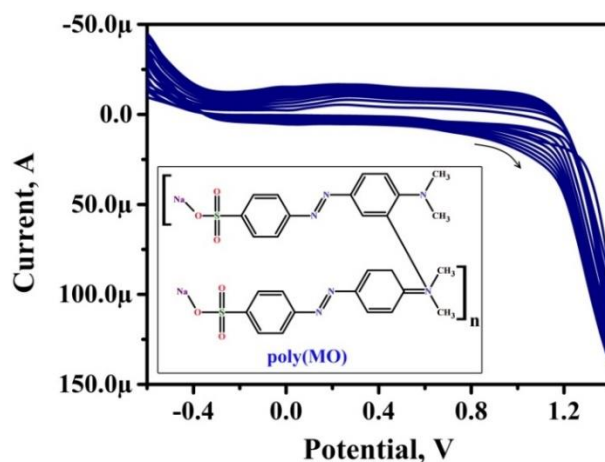


Figure 1. CVs obtained for the electropolymerization of 1 mM MO in 0.2 M PBS of pH 7.0 at a scan rate of 0.1 V/s on the BCNTPE surface for 10 cycles

3. RESULTS AND DISCUSSIONS

3.1 Electrochemical activity of PMO/CNTPE and BCNTPE towards the redox probe ferrocyanide

The conventional CVs for 1 mM $[\text{Fe}(\text{CN})_6]^{3-/4-}$ in 0.1 M KCl within the potential gap of -0.2 V to 0.6 V (at 0.1 V/s) at PMO/CNTPE (trace a) and BCNTPE (trace b) have been shown in Fig. 2. From the assessment, the anodic peak current (I_{pa}) at BCNTPE and PMO/CNTPE were varied predominantly with value of 8.32 μA and 44.01 μA , respectively. Moreover, the peak occurred at the potential of 0.18 V via PMO/CNTPE was less in contrast to that of the peak observed at BCNTPE (i.e. 0.265 V). This improved activity of PMO/CNTPE is due to the enhancement in the area of active sites at the electrode surface and it was evaluated through the Randles-Sevcik expression as follows [27–30],

$$I_p = 2.69 \times 10^5 n^{3/2} A D^{1/2} \nu^{1/2} C \quad (1)$$

Here, I_p = peak current, n = quantity of electrons involved, A = area of electroactive surface, D = co-efficient of diffusion, ν = scan rate, C = concentration of redox probe solution. By the use of these data, A was assessed to be 0.012 cm^2 for BCNTPE and 0.059 cm^2 for PMO/CNTPE.

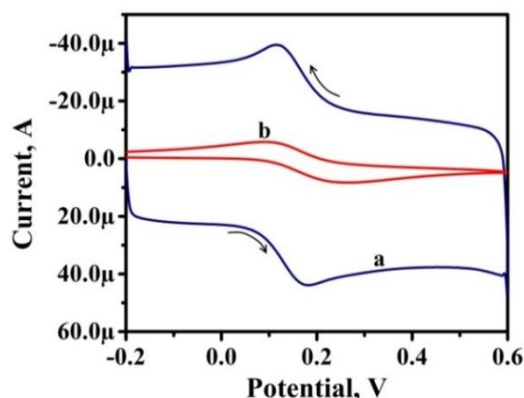


Figure 2. CVs of 1 mM $[\text{Fe}(\text{CN})_6]^{3-/4-}$ at BCNTPE (trace b) and PMO/CNTPE (trace a) in 0.1 M KCl at a scan rate of 0.1 V/s

3.2 Electrode surface characterization by FE-SEM

FE-SEM images were used to characterize the surface of BCNTPE and PMO/CNTPE and the collected images are shown in Fig. 3. Fig. 3a presents the surface structure of BCNTPE, which shows irregularly scattered strands of MWCNTs. In contrast to that, the surface structure of PMO/CNTPE (Fig. 3b) shows a smooth texture due to the formation of a polymer layer. The developed layer makes the electrode surface more even and uniform, which enhances the surface features of the polymerized electrode for the sensing of target analyte.

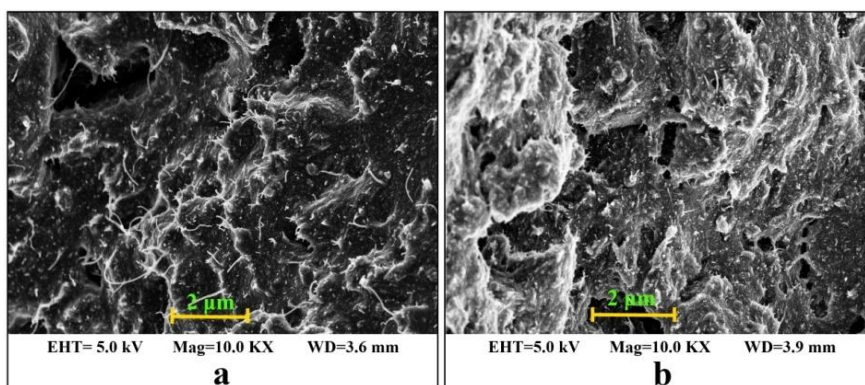


Figure 3. FE-SEM images of a) BCNTPE b) PMO/CNTPE

3.3 EIS study

Fig. 4 presents the Nyquist plot of EIS on BCNTPE (trace a) and PMO/CNTPE (trace b) for 1 mM $[\text{Fe}(\text{CN})_6]^{3-/4-}$ in 0.1 M KCl in the ac frequency range from 1 Hz to 1000 kHz. The PMO/CNTPE presents the less charge transfer resistance ($R_{ct}=10.21 \text{ k}\Omega$) than BCNTPE ($R_{ct}=11.77 \text{ k}\Omega$) owing to the better electronic property of the polymer layer. Also, it was further confirmed by the study of semicircles formed in the EIS curve.

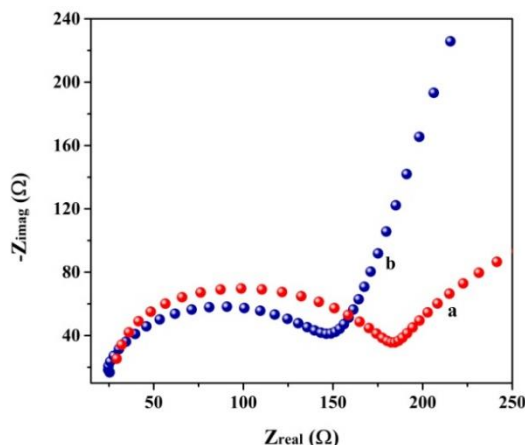


Figure 4. Nyquist plots of 1 mM $[\text{Fe}(\text{CN})_6]^{3-/4-}$ in 0.1 M KCl at BCNTPE (trace a) and PMO/CNTPE (trace b)

Larger the semicircle lesser the conduction property, here we found the larger semicircle for BCNTPE confirms the less conductivity of the electrode compared to PMO/CNTPE. Furthermore, the conductance of the developed sensor was also evaluated by fitting the obtained data to the equivalent circuit and it was obtained as $1.01 \mu\text{F}$ for BCNTPE and $9.53 \mu\text{F}$ for PMO/CNTPE. These results confirm the successful development of poly(MO) coating on the BCNTPE surface.

3.4 Influence of pH

The pH effect on the CTZ (0.1 mM) electro-oxidation was studied at the PMO/CNTPE in 0.2 M supporting buffer (PBS) of various pH over the range from 5.5 to 8.0 via CV method at 0.1 V/s. As illustrated in Fig. 5a, a firm and well-defined irreversible anodic peaks were produced on the CVs and the emergence of two anodic signals is due to the CTZ dimerization. Since the first analytical signal is of more sensitive and sharp, it was considered for the remaining electrochemical study.

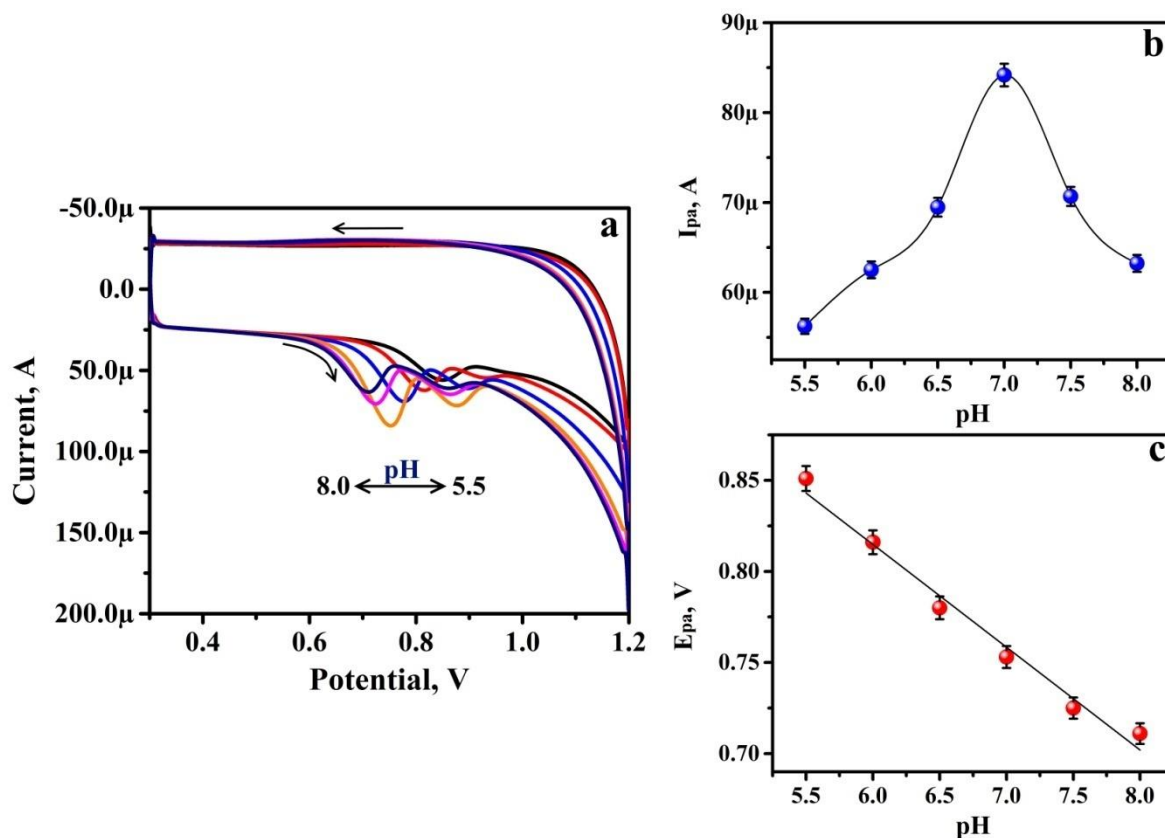


Figure 5. a) CVs for 0.1 mM CTZ at PMO/CNTPE in 0.2 M PBS at different pH values from 5.5 to 8.0 b) Plot of I_{pa} vs. pH c) Plot of E_{pa} with respect to pH

The corresponding plot of I_{pa} at various pH is portrayed in Fig. 5b. As observed from this, the I_{pa} was gradually upsurges with the rise in pH from 5.5 to 7.0 and then decreased with the increase of pH. Considering this outcome, the physiological pH 7.0 was preferred as optimal for further study. The

relationship of the potential of anodic peak (E_{pa}) with different pH buffer was constructed with the achieved results as delineated in Fig. 5c. As the pH increases the corresponding E_{pa} gradually shifted linearly towards a lower positive region. This variation in potential at different pH is because of the protonation and deprotonation reaction of CTZ at different pH buffer. The regression equation related to this linearity can be expressed as,

$$E_{pa} \text{ (V)} = 1.153 - 0.056 \text{ pH (V/pH)} \quad R=0.995 \quad (2)$$

The obtained slope value of 0.056 V/pH is very closer to the tentative Nernstian value 0.059 V/pH signifying that the overall CTZ reaction is proceed through the involvement of equal proportion of electrons and hydrogen ions [31–34].

3.5 Influence of scan rate

The scan rate effect on the electro-activity of CTZ was assessed by CV method by varying scan rate from 0.075 to 0.25 V/s in PBS of pH 7.0 at PMO/CNTPE (Fig. 6a). The I_{pa} concerning CTZ electro-oxidation was increased linearly with the progression of scan rate, showcasing that the kinetics of electron transfer using CV is the characteristic of the adsorption controlled phenomena [35]. The plot corresponding to this relation is illustrated in Fig. 6b and the linear fit Eq. related to this is,

$$I_{pa} \text{ (}\mu\text{A)} = -1.048 + 587.78 \nu \text{ (V/s)} \quad R=0.993 \quad (3)$$

Furthermore, the adsorption controlled phenomena of the electrode was further confirmed by the study of relation between $\log I_{pa}$ and $\log \nu$ (Fig. 6c). The linear expression of this relationship is,

$$\log (I_{pa}, \mu\text{A}) = 2.737 + 0.980 \log (\nu, \text{V/s}) \quad R=0.995 \quad (4)$$

The slope value of this relationship 0.98 is very closer to the expected value 1.0 for the adsorption controlled phenomena [36].

So as to evaluate the number of electrons (n) involved in the CTZ electrochemical reaction, the following Laviron equation (Eq. 5) was utilized [37].

$$E_{pa} = K + \frac{2.303RT}{\alpha nF} \log \nu \quad (5)$$

To acquire the slope of the relation between E_{pa} and $\log \nu$, the respective graph was plotted (Fig. 6d) and the linear equation of this relationship is,

$$E_{pa} \text{ (V)} = 0.872 + 0.119 \log (\nu, \text{V/s}) \quad R=0.982 \quad (6)$$

With the application of coefficient of charge transfer ($\alpha:0.5$ for the irreversible process) and the slope of E_{pa} vs. $\log \nu$ in Eq. 5, the value of n was deliberate as $0.99 \approx 1.0$, which is in close agreement with the reported work for CTZ [38]. The mechanism of electro-oxidation of CTZ is described in Scheme 1.

The concentration of CTZ at PMO/CNTPE surface (Γ) was also evaluated using the following equation (eq. 7) [39],

$$\Gamma = \frac{Q}{nFA} \quad (7)$$

Here Q defines the integrated charge of oxidation peak at 0.1 V/s and the remaining symbols defines their standard meaning. From Eq. 7, the value of Γ was evaluated as 2.88 nmol/cm².

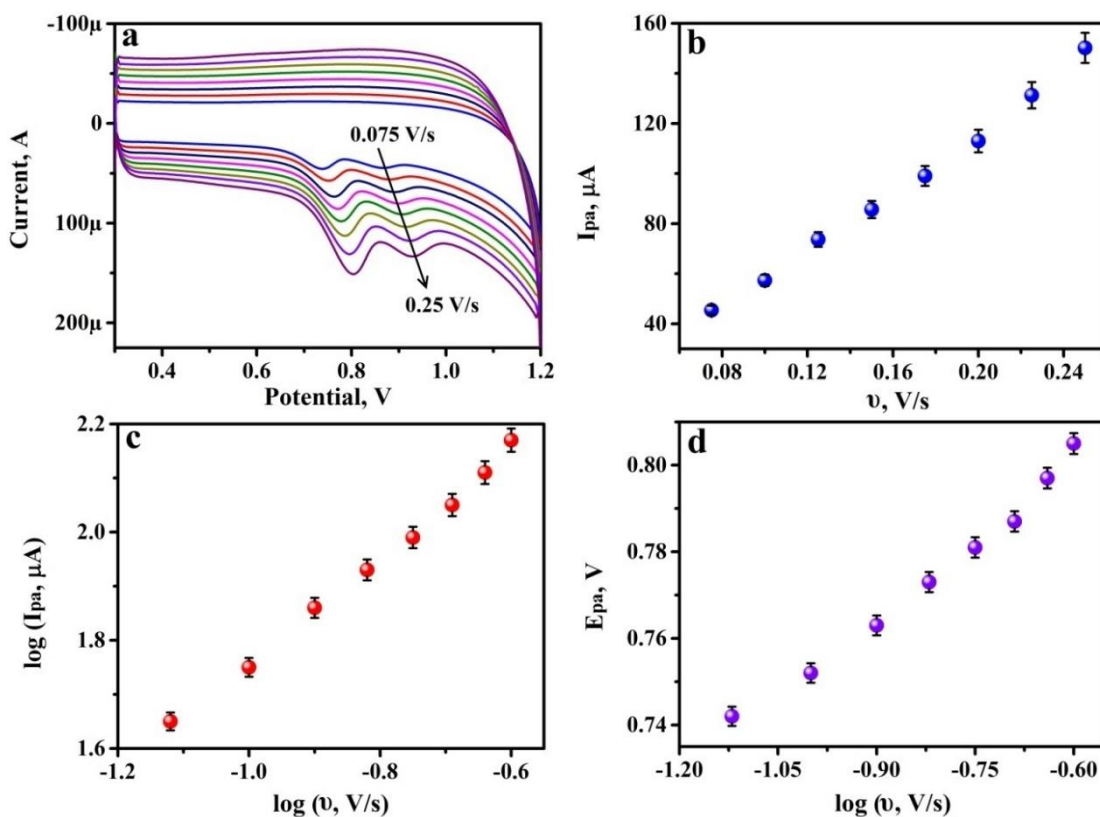
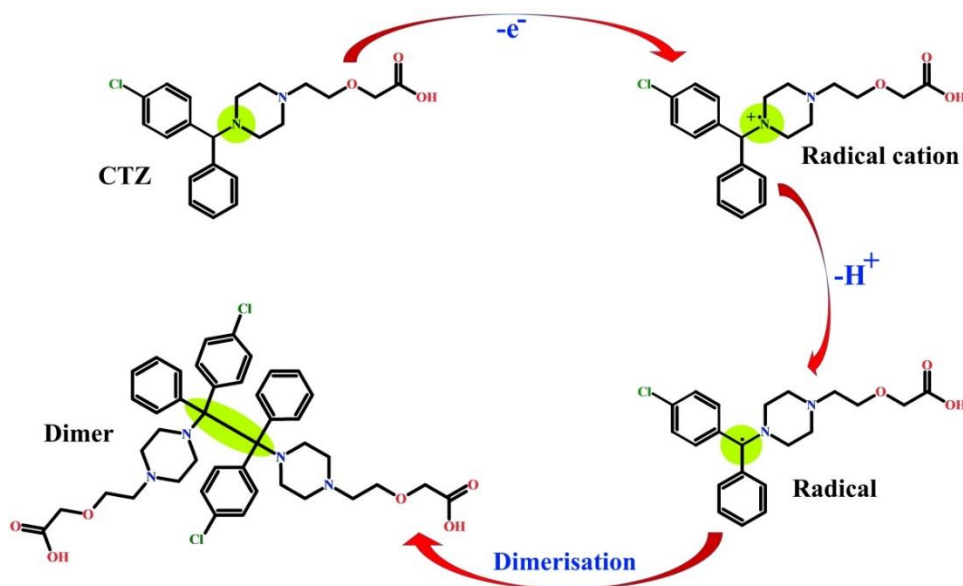


Figure 6. a) CVs for 0.1 mM CTZ at PMO/CNTPE in 0.2 M PBS of pH 7.0 at various scan rates from 0.075-0.25 V/s b) Graph of I_{pa} vs. scan rate c) Graph of $\log I_{pa}$ vs. $\log v$ d) Graph of E_{pa} vs. $\log v$



Scheme 1. Electro-oxidation mechanism of CTZ

3.6 Electrochemical activity of CTZ

The CV responses of 0.1 mM CTZ in 0.2 M PBS (pH 7.0) at the BCNTPE (trace b) and PMO/CNTPE were shown in Fig. 7. A well defined oxidation peaks were appeared at 0.75 V and 0.87

V at PMO/CNTPE for CTZ electro-oxidation. Whereas the nonappearance of reduction peak in the CVs indicating that the CTZ electrochemical reaction was totally irreversible at the designed electrode surface. Furthermore, the I_{pa} of 0.1 mM CTZ at the PMO/CNTPE ($84.18 \mu\text{A}$) was around 10 times larger than that of the BCNTPE ($7.28 \mu\text{A}$). Also the investigational results exhibited that the E_{pa} of CTZ was greatly decreased at the PMO/CNTPE in contrast to the BCNTPE. The poly(MO) layer on the electrode exterior presents an admirable electrocatalytic performance towards CTZ oxidation, which accelerates the transfer of electrons and produced the enhanced analytical response for CTZ. The CV response was also obtained for 0.2 M PBS (pH 7.0) in the absence of CTZ (trace c) and it does not showed any peak response.

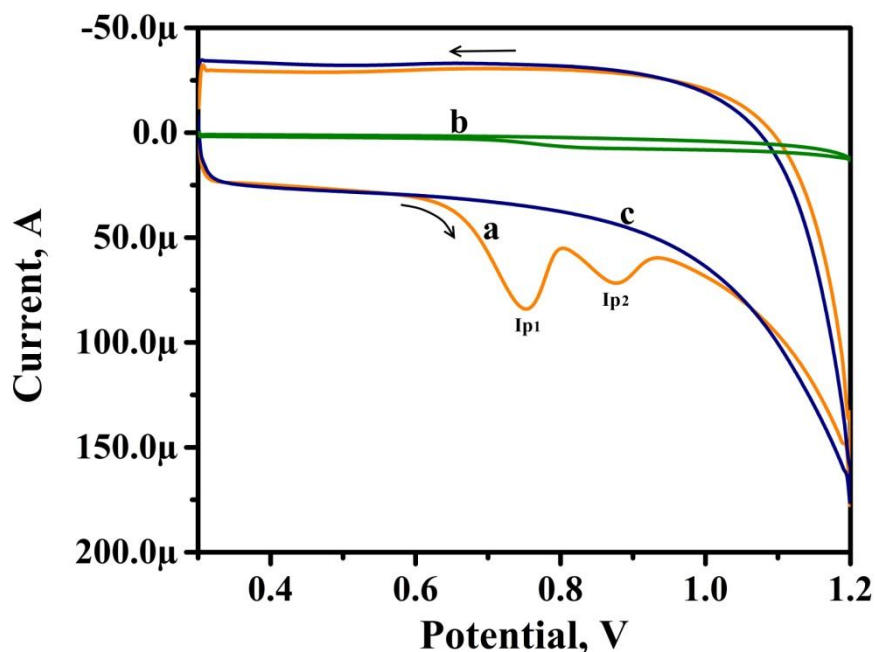


Figure 7. CVs of 0.1 mM CTZ at BCNTPE (trace b) and PMO/CNTPE (trace a) at PBS of pH 7.0. CV response for PBS of pH 7.0 (trace c) at PMO/CNTPE

3.7 Simultaneous analysis of CTZ and PCM

Due to the medicinal importance and the coexistence of PCM and CTZ in most of the medication these were determined simultaneously at PMO/CNTPE and BCNTPE. The CV response of varied concentrations of PCM and CTZ were collected in 0.2 M PBS of pH 7.0 at PMO/CNTPE (Fig. 8, trace b). The CV response obtained at BCNTPE (trace a) was negligible compared to the response produced by the modified electrode. From the acquired CVs we seen that as the concentration of PCM and CTZ increased the I_{pa} relating to the electro-oxidation of both the analytes were increased and the I_{pc} with respect to PCM reduction was also increased gradually. It proves that the developed electrode was capable of determining PCM and CTZ

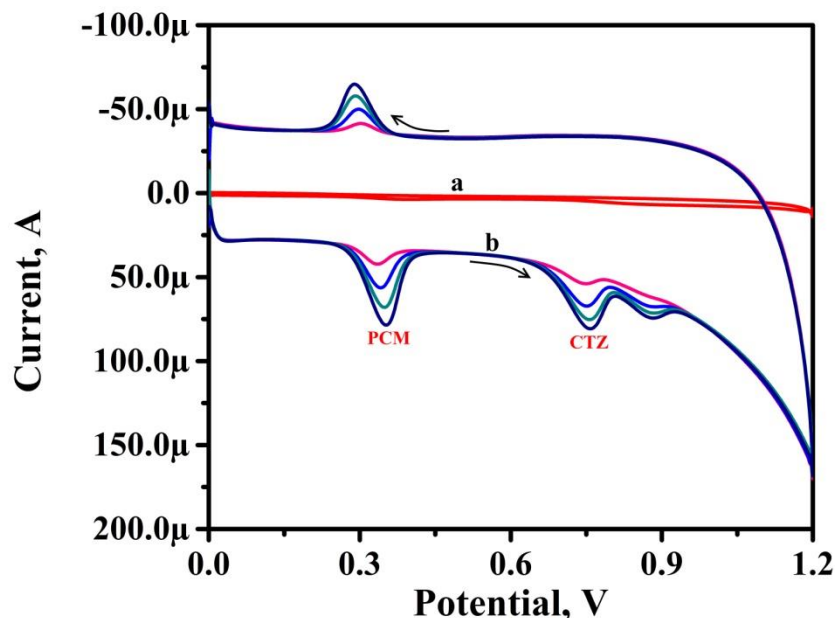


Figure 8. CVs of various concentrations of PCM and CTZ in 0.2 M PBS of pH 7.0 at PMO/CNTPE

3.8 Repeatability, reproducibility and stability of PMO/CNTPE

The PMO/CNTPE was checked for its repeatability, reproducibility and stability through CV technique. The repeatability of PMO/CNTPE was evaluated by obtaining the relative standard deviation (RSD) of the I_{pa} for unique concentration of CTZ ($N=5$) and it was obtained as 1.58 %. The reproducibility of the PMO/CNTPE was studied by obtaining the CV response at five independent electrodes prepared under optimized conditions. The obtained RSD (2.22 %) exposes the excellent reproducibility of the electrode. The long-term stability of the PMO/CNTPE towards CTZ detection was investigated through CV for 1 week. The I_{pa} obtained after 1 week was 88.84 % of its initial value presents the excellent stability of the designed electrode.

3.9 Evaluation of limit of detection

The CV signals produced for examined various concentrations of CTZ in 0.2 M PBS (pH 7.0) at PMO/CNTPE is shown in Fig. 9a. It is worth observing that the I_{pa} values corresponding to the oxidation of CTZ increased gradually with the enhancement in CTZ concentration and the corresponding plot is shown in Fig. 9b. Two linear curves were obtained in the range of concentration of 2 μM to 10 μM and from 10 μM to 45 μM . The slope of second linearity (10 μM to 45 μM) was taken for the calculation of limit of detection (LOD) and limit of quantification (LOQ) of CTZ at PMO/CNTPE. The equation of linearity of the calibration plot can be expressed as,

$$I_{pa} (\mu\text{A}) = 3.75 \times 10^{-5} + 0.71 C (\text{M}) \quad R = 0.995 \quad (8)$$

The LOD and LOQ were evaluated using the slope of this linear plot and the standard deviation of the blank assessments ($N=5$) and it was obtained as 0.076 μM and 0.25 μM , correspondingly.

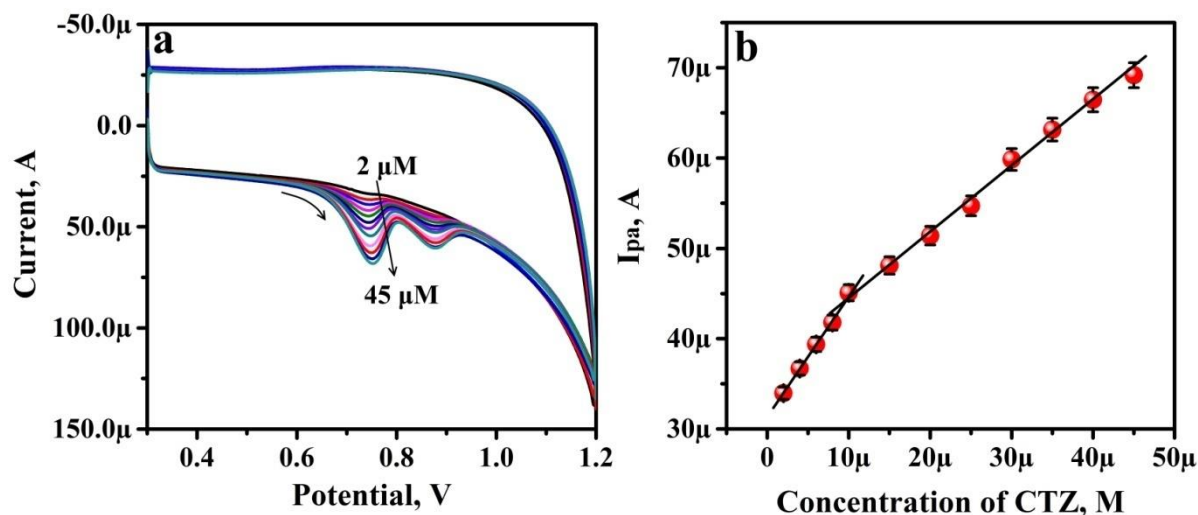


Figure 9. a) CVs obtained by increasing the concentrations of CTZ at PMO/CNTPE in 0.2 M PBS pH 7.0 b) Plot of I_{pa} versus various concentration of CTZ

The accomplished results were compared with the other reported results for the investigation of CTZ at different electrodes and the data were summarised in Table 1.

Method	Electrode	Linear range (μM)	LOD (μM)	Reference
DPV	BDDE	67–540	0.016	[38]
AdS.DPV	MWCNT–Pt–CPE	0.19–193	0.058	[12]
CV	MWCNT–GCE	0.5–10	0.071	[13]
SWV	p–GP	0.5–10	0.16	[40]
SWAdASV	CB–GCE	0.49–10.8	0.40	[41]
CV	PLMCNTPE	5–50	0.17	[42]
CV	CTABMCNTPE	10–100	0.27	[43]
CV	PVLMCNTPS	2–80	0.11	[44]
CV	PMO/CNTPE	2–45	0.076	[This work]

3.10 Analysis of pharmaceutical sample

With the intension to examine the analytical applicability of the developed electrode and the utilized method, it was applied for the analysis of CTZ in CTZ tablets. The tablets under investigation was crushed into fine powder and prepare a solution of known concentration by using 0.2 M PBS . Then the solution was filtered through Whatman filter paper to remove the undissolved particles. The supernatant liquid was used for the analysis. The results acquired from the analysis is tabulated in Table 2.

Table 2. Recovery data of CTZ tablet sample

CTZ tablet sample	Added (μM)	Found (μM)	Recovery (%)
	6.00	5.95	99.31
	10.00	9.80	98.04
	15.00	14.72	98.17

4. CONCLUSIONS

MWCNTs and the layer of poly(MO) produced a high sensitive electrode for CTZ analysis. The electrochemical activity of CTZ on the surface of PMO/CNTPE was investigated in 0.2 M PBS of pH 7.0. The electrode characteristics were explored using CV, EIS and FE-SEM data. Under the experimental circumstances, the I_{pa} is linear to CTZ concentration in the range from 10 μM to 45 μM , and the LOD was obtained as 0.076 μM . The designed electrode provides advantages like high sensitivity, easy preparation, low cost, real sample applicability, and stability. The experimental outcome reveal the utility of electrode and the method for the analysis of CTZ in tablet sample without any further extraction step, purification and derivatization.

ACKNOWLEDGEMENTS

The authors acknowledge the Deanship of Scientific Research at King Faisal University, Kingdom of Saudi Arabia for their financial support under Nasher Track (Grant No. 206032) and their encouragement.

References

1. S. Martindale. The complete drug reference 33. ed., The Pharmaceutical Press, London, (2002) p. 411.
2. A. Einarson, B. Bailey B, G. Jung, D. Spizzirri, M. Baillie, G. Koren, *Ann. Allergy, Asthma, Immunol.*, 78 (1997) 183.
3. M. Mircarini, M. Pasquali, C. Cosentino, F. Fumagalli, A. Scordamaglia, R. Quaglia, G. W Canonica, G. Passalacqua, *Pulm. Pharmacol. Ther.*, 14 (2001) 267.
4. S. Rudaz, S. Souverain, C. Schelling, M. Deleers, A. Klomp, A. Norris, T.L. Vu, B. Ariano, J.L. Veuthey, *Anal. Chim. Acta*, 492 (2003) 271.
5. S.N. Makhija, P.R. Vavia, *J. Pharm. Biomed. Anal.*, 25 (2001) 663.
6. N. Kristiningrum, M.E. Novita, *Int. Curr. Pharm. J.*, 3 (2013) 208.
7. A.M.Y. Jaber, H.A. Al-Sherife, M.M. Al-Omari, A.A. Badwan, *J. Pharm. Biomed. Anal.*, 36 (2004) 341.
8. H. Mahgoub, A.A. Gazy, F.A. El-Yazbi, M.A. El-Sayed, R.M. Youssef, *J. Pharm. Biomed. Anal.*, 31 (2003) 801.
9. E. Baltés, R. Coupez, L. Brouwers, J. Gobert, *J. Chromatogr.*, 430 (1988) 149.
10. J.F. Sattary, A. Shafaat, A. Zarghi, *J. Anal. Chem.*, 69 (2014) 442.
11. H. Eriksen, R. Houghton, R. Green, J. Scarth, *Chromatographia*, 55 (2002) S145.
12. P.K. Kalambate, A.K. Srivastava, *Sens. Actuators B Chem.*, 233 (2016) 237.
13. R.H. Patil, R.N. Hegde, S.T. Nandibewoor, *Colloids Surf. B.*, 83 (2011) 133.

14. P.A. Pushpanjali, J.G. Manjunatha, B.M. Amrutha, N. Hareesha, *Mater. Res. Innov.*, 25 (2021) 412.
15. H. M. Moghaddam, H. Beitollahi, S. Tajik, S. Jahani, H. Khabazzadeh, R. Alizadeh, *Russ. J. Electrochem.*, 53 (2017) 515.
16. T. Girish, J.G. Manjunatha, E.S. D'Souza, N. Sreeharsha, *ChemistrySelect*, 6 (2021) 2700.
17. M. Ibrahim, H. Ibrahim, N. Almandil, A.-N. Kawde, *Sens. Actuators B Chem.*, 274 (2018) 123.
18. J.G. Manjunatha, *Open Chem. Eng.*, 14 (2020) 52.
19. L. Agui, P. Yanez-Sedeno, J.M. Pingarron, *Anal. Chim. Acta*, 622 (2008) 11.
20. P.A. Pushpanjali, J.G. Manjunatha, *Phys. Chem. Res.*, 7 (2019) 813.
21. N.S. Prinith, J.G. Manjunatha, *Mater. Res. Innov.*, (2021) 1.
22. J.J. Gooding, *Electrochim. Acta*, 50 (2005) 3049.
23. P.A. Pushpanjali, J.G. Manjunatha, *Electroanalysis*, 32 (2020) 2474.
24. B.M. Amrutha, J.G. Manjunatha, A.S. Bhatt, N. Hareesha, *J. Sci. Adv. Mater. Devices*, 6 (2021). 415.
25. P.K. Bairagi, N. Verma, *J. Electroanal. Chem.*, 814 (201)134.
26. N. Hareesha, J.G. Manjunatha, *J. Iran. Chem. Soc.*, 17 (2020)1507.
27. P.A. Pushpanjali, J.G. Manjunatha, M.T. Srinivas, *FlatChem.*, 24 (2020) 100207.
28. H. Ibrahim, Y. Temerk, *Talanta*, 208 (2020) 120362
29. B.T. Harshitha, J.G. Manjunatha, P.A. Pushpanjali, C.S. Karthik, S. Sandeep, P. Mallu, Edwin D'Souza, N. Sreeharsha, S.M. Basheeruddin Asdaq, M.K. Anwer, *ChemistrySelect*, 6 (2021) 6764.
30. B.M. Amrutha, J.G. Manjunatha, A.S. Bhatt, P.A. Pushpanjali, *J. Food Meas. Charact.*, 6 (2020) 3633.
31. N. Hareesha, J.G. Manjunatha, *Sci. Rep.*, 11 (2021) 12797.
32. M.M. Charithra, J.G. Manjunatha, N.S. Prinith, P.A. Pushpanjali, T. Girish, N. Hareesha, *Mater. Res. Innov.*, (2021) 1.
33. J.G. Manjunatha, *Chem. Data. Coll.*, 25 (2020) 100331.
34. J.G. Manjunatha, M. Deraman, *Anal. Bioanal. Electrochem.*, 9 (2017) 198.
35. N. Hareesha, J.G. Manjunatha, B.M. Amrutha, P.A. Pushpanjali, M.M. Charithra, N. Prinith Subbaiah, *J. Electron. Mater.*, 50 (2021)1.
36. P.A. Pushpanjali, J.G. Manjunatha, M.T. Srinivas, *FlatChem.*, 24 (2020) 100207.
37. E. Laviron, *J. Electroanal. Chem. Interf. Electrochem.*, 101 (1979) 19.
38. E. Culková, Z. Lukáčová-Chomisteková, R. Bellová, D. Melicherčíková, J. Durdiak, J. Timko, M. Rievaj, P. Tomčík, *Int. J. Electrochem. Sci.*, 13 (2018) 6358.
39. H. Razmi, M. Harasi, *Int. J. Electrochem. Sci.*, 3 (2008) 82.
40. S. Karakaya, D.G. Dilgin, *Monatsh. Chem.*, 150 (2019) 1003.
41. B.C. Lourencao, T.A. Silva, M. da Silva Santos, A.G. Ferreira, O. Fatibello-Filho, *J. Electroanal. Chem.*, 807 (2017) 187.
42. P.A. Pushpanjali, J.G. Manjunatha, N. Hareesha, E.S.D. Souza, M.M. Charithra, N.S. Prinith, *Surf. Interfaces*, 24 (2021)101154.
43. P.A. Pushpanjali, J.G. Manjunatha, N. Sreeharsha, S.M. Basheeruddin Asdaq, M.K. Anwer, *J. Mater. Sci Mater. Electron.*, 32 (2021) 22668.
44. T. Girish, J.G. Manjunatha, P.A. Pushpanjali, N.S. Prinith, D.K. Ravishankar, G. Siddaraju, *J.E.S.E.*, 11 (2021) 27.